

Cytotoxic and Antiproliferative Effects of β -Mangostin on Rat C6 Glioma Cells Depend on Oxidative Stress Induction via PI3K/AKT/mTOR Pathway Inhibition

This article was published in the following Dove Press journal:
Drug Design, Development and Therapy

Kaiqiang Li,^{1,3,*}
Lingling Wu,^{1,*} Yili Chen,^{4,*}
Yuanyuan Li,⁵
Qianni Wang,¹ Min Li,³
Ke Hao,^{2,3} Wei Zhang,³
Shanshan Jiang,²
Zhen Wang^{1,2}

¹School of Laboratory Medicine and Life Sciences, Wenzhou Medical University, Wenzhou 325027, People's Republic of China; ²Research Center of Blood Transfusion Medicine, Ministry of Education Key Laboratory of Laboratory Medicine, Zhejiang Provincial People's Hospital, People's Hospital of Hangzhou Medical College, Hangzhou 310014, People's Republic of China; ³Rehabilitation & Sports Medicine Research Institute of Zhejiang Province, Zhejiang Provincial People's Hospital, People's Hospital of Hangzhou Medical College, Hangzhou 310014, People's Republic of China; ⁴College of Pharmaceutical Science, Zhejiang University of Technology, Hangzhou 310014, People's Republic of China; ⁵School of Pharmacy, Hangzhou Medical College, Hangzhou 310014, People's Republic of China

*These authors contributed equally to this work

Correspondence: Shanshan Jiang;
Zhen Wang
Zhejiang Provincial People's Hospital,
People's Hospital of Hangzhou Medical
College, Hangzhou 310014, People's
Republic of China
Tel +86 571-87666666
Fax +86 571-85131448
Email jiangss-1982@163.com;
wangzhen@hmc.edu.cn

Background: Glioma is the most common malignant tumor of the nervous system, which accounts for more than 45% of central nervous system tumors and seriously threatens our health. Because of high mortality rate, limitations, and many complications of traditional treatment methods, new treatment methods are urgently needed. β -Mangostin is a natural compound derived from the fruit of *Garcinia mangostana* L. and it has anticancer activity in several types of cancer cells. However, the antitumor effect of β -mangostin in glioma has not been clarified. Hence, this study aimed to investigate its therapeutic effects on gliomas.

Materials and Methods: To study the effect of β -mangostin on glioma cells, cell viability assay, reactive oxygen species production, cell cycle, apoptosis, and mitochondrial membrane potential were evaluated in the C6 cell line in vitro. Immunofluorescence and Western blotting were used to analyze protein expression and phosphorylation to study its mechanism of action. A subcutaneous xenograft model was used to investigate the effect of β -mangostin on tumorigenesis in vivo.

Results: We found that β -mangostin can inhibit glioma cell growth and induce oxidative damage in vitro. In addition, it reduces the phosphorylated form levels of PI3K, AKT and mTOR. Furthermore, the phosphorylated form levels of PI3K, AKT and mTOR were increased after the PI3K inhibitor was added. In vivo experiments showed that β -mangostin can inhibit tumor growth as shown by its reduced size and weight.

Conclusion: This study suggests that β -mangostin can inhibit cell proliferation and induce oxidative damage in cells. It is the first study to demonstrate that β -mangostin induces oxidative damage in glioma cells by inhibiting the PI3K/AKT/mTOR signaling pathway.

Keywords: glioma, PI3K/AKT/mTOR, oxidative damage, *Garcinia mangostana* L.

Introduction

Gliomas are the most common primary intracranial tumors and prognosis remains dismal despite the optimal treatment approach developed for this disease.¹ The median survival time in patients with newly diagnosed glioblastoma (GBM) is frequently less than 15 months, and the 5-year survival rate in patients is about 5%.^{2,3} Temozolomide (TMZ) is the first-line chemotherapeutic drug for glioma treatment with a definite curative effect.⁴ However, its efficacy is frequently limited by the durability of the chemoresistance response.^{5,6} Thus, the development of innovative drugs is urgently needed to prevent the recurrence and distal metastasis of GBM and prolong the survival in glioma patients.

Garcinia mangostana L., also known as mangosteen whose fruits have been used in traditional medicine to treat several conditions for centuries, is an evergreen tree native to Southeast Asia.⁷ Mangosteen fruit shells contain a variety of xanthone derivatives, mainly including α -mangostin, β -mangostin and γ -mangostin. Previous reports have demonstrated that extracts of mangosteen have antitumoral,^{8,9} antioxidant,^{10–12} antiallergic,¹³ anti-inflammatory,^{14,15} antibacterial,¹⁶ and antiviral activities.¹⁷ β -Mangostin are xanthenes, which have anticancer activity against several types of cancer cells, including hepatocellular carcinoma cells,¹⁸ melanoma cells,¹⁹ and cervical cancer cells.²⁰ However, the anticancer effect of β -mangostin on glioma is still ambiguous.

A growing evidence indicates that reactive oxygen species (ROS) generation is one of the important mechanisms underlying the chemotherapy drug effects in glioma.²¹ Specifically, α -mangostin induces apoptosis through activation of ROS and ASK1/p38 signaling pathway in cervical cancer cells. It was shown in HL60 cells that β -mangostin from *Cratoxylum arborescens* activated intrinsic apoptotic pathway through activation of ROS by downregulation of the HSP70 gene.²² However, it is not known if mangostin is effective in treating gliomas. In this study, we aimed to explore the anticancer effect of β -mangostin on glioma, with particular attention to the potential molecular mechanisms of oxidative damage. Furthermore, we tried to provide a theoretical basis for the drug treatment of cancer.

Materials and Methods

Plant Material

Garcinia mangostana L. were obtained from Thailand in October 2018. Full publication details for this name can be found in IPNI: <http://ipni.org/urn:lsid:ipni.org:names:428073-1>.

Extraction of β -Mangostin from *Garcinia mangostana* L

Garcinia mangostana L. were obtained from Thailand in October 2018. Fresh pericarps were separated and dried in a ventilated room for a week. The air-dried peel was crushed into fine powder. The powder (2.4 kg) was immersed in ethanol (8 L) three times for 7 days and the supernatant was collected. The three supernatants were dried with a rotary evaporator to obtain the total extract (175 g). This was then extracted with water and

chloroform, and the chloroform fraction was collected and dried. Afterwards, column chromatography was used to roughly separate the extract into six components, with petroleum ether and ethyl acetate (from 8:1, 5:1, 3:1, to 1:1 v/v) as mobile phases. The third component was subdivided into further fractions and eluted with a gradient of petroleum ether and ethyl acetate (from 8:1 to 5:1, v/v) to separate its main component.

Cell Culture and β -Mangostin Treatment

Rat C6 glioma cells were obtained from the Chinese Academy of Sciences Cell Bank (Shanghai, China), and were cultured in DMEM (Hyclone, Shanghai, China) medium supplemented with 10% v/v fetal bovine serum (FBS, Gibco, USA), 100 U/mL penicillin, and 100 μ g/mL streptomycin. Cells were maintained and grown in a humidified incubator with 5% CO₂. The cells were treated with β -mangostin which was dissolved in 0.1% dimethyl sulfoxide (DMSO, SigmaAldrich, Shanghai, China), and cells treated with 0.1% DMSO alone were set as a control.

Cell Viability Assay

CCK-8 assay was used to measure cell viability. C6 cells were seeded at 5×10^3 cells/well in 96-well plates (100 μ L/well). After 24 h, the cells were treated with various concentrations of β -mangostin (0 to 25 μ M) for 24 h. After incubation, 10 μ L of CCK-8 solution (Beyotime, Shanghai, China) was then added, and the cells were incubated for 2 h. The absorbance was monitored at 450 nm using a microplate reader.

Colony Formation Ability Assay

About 5×10^2 C6 cells were seeded in 6-well plates. The C6 cells were pretreated with four different concentrations of β -mangostin (0, 6.25, 12.5, 25 μ M) for 24 h. Subsequently, the medium was changed in the culture for the next 7 days. Afterwards, C6 cells were washed with PBS and fixed in 4% paraformaldehyde (Sigma, USA) for 10 min and stained with crystal violet (Meilunbio, Dalian, China) for 20 min at room temperature. Lastly, GraphPad Prism 8 (GraphPad Software, Inc.) was used to perform statistical analysis of colony formation ability results.

Scratch Assay

Cells were grown in 6-well plates. After reaching 80% confluence, a scratch was made using a pipette tip. After changing the medium, cells were incubated in a new medium containing 1% FBS with mitomycin C (Selleck,

Shanghai, China), and the images of the scratch region were captured at 0 and 24 h using a microscope (Nikon, Tokyo, Japan).

Intracellular ROS Generation

Intracellular ROS accumulation was measured using the ROS Assay Kit (Beyotime). C6 cells were seeded in 6-well plates and treated with β -mangostin (0, 6.25, and 12.5 μ M) for 24 h. Cells were stained with 10 μ M DCF-DA for 20 min at 37°C and washed three times with PBS for detection. Lastly, cells were harvested by fluorescence microscope (Nikon, Tokyo, Japan), and analyzed by flow cytometry.

Detection of the Mitochondrial Membrane Potential

The mitochondrial membrane potential was visualized using 5,5',6,6'-tetrachloro-1,1',3,3' tetraethyl-imidacarbocyanine iodide (JC-1, Beyotime, Shanghai, China) staining. C6 cells were seeded into 6-well plates at a density of 2×10^5 /well and cultured for 24 h. After 24 h of treatment with β -mangostin, cells were harvested and incubated with JC-1 for 15 min at 37°C. After washing off the dye, the cells were immediately analyzed using flow cytometry.

Flow Cytometry Analysis of Apoptosis

C6 cells were seeded in 6-well plates for 24 h and pre-treated with three different concentrations of β -mangostin (0, 6.25, 12.5 μ M). The induction of apoptosis was assessed by Annexin V-FITC/PI Apoptosis Detection Kit (Beyotime, Shanghai, China). Tests were carried out in accordance with the manufacturer's instructions. Finally, the cells were harvested and immediately analyzed using flow cytometry.

Cell Cycle Analysis

The role of β -mangostin in cell cycle profiles was monitored using flow cytometry with PI/RNase staining buffer. Briefly, the cells were seeded in 6-well plates at a density of 3×10^5 cells/well for 24 h. Cells were then harvested and fixed with 70% (v/v) ethanol. DNA was stained with a PI (3,8-diamino-5-[3-(diethylmethylammonio)propyl]-6-phenyl-phenanthridinium diiodide) staining solution for at least 10 min at room temperature in the dark. Fluorescence intensity was measured using flow cytometry in combination with NovoExpress software.

Western Blotting

Briefly, an equivalent amount of protein (20 μ g) from each sample was separated on 10% SDS-PAGE and transferred to the PVDF membrane (Millipore, Billerica, MA). The membranes were blocked with 5% nonfat dry milk for 1 h and then incubated with the respective primary antibodies overnight at 4°C. The antibodies included PI3K (CST, Shanghai, China), p-PI3K (CST, Shanghai, China), AKT (CST, Shanghai, China), p-AKT (CST, Shanghai, China), mTOR (CST, Shanghai, China), p-mTOR (CST, Shanghai, China), and GAPDH (Huaan, Hangzhou, China). Afterwards, the membranes were incubated with HRP-conjugated secondary antibody (Huaan, Hangzhou, China). After the washing step, protein bands were visualized using the ECL reagent (Beyotime, Shanghai, China) and captured using the Bio-Rad image system (Bio-Rad, California, USA). Protein bands were analyzed using ImageJ software, and the results were normalized to GAPDH levels in each lane.

Animal Experiments

All experimental procedures and protocols were reviewed and ethically approved by the Animal Care and Use Committee of Zhejiang Provincial People's Hospital and were in accordance with the Guide for the Use and Care of Laboratory Animals. All animals were raised in SPF level environment and all animal experiments were undertaken while following a robust ethical review. Male BALB/c nude mice (specific pathogen-free grade, 4 weeks old, 18–20 g) were obtained from Slake Laboratory Animal Company (Shanghai, China). The mice were housed at $23 \pm 1^\circ\text{C}$ on a standard 12:12-hour light/dark cycle, with water and food pellets available ad libitum. Tumors were implanted by subcutaneous injection of 1×10^6 C6 cells in 100 μ L of PBS into the right back of each mice. Tumor volume was calculated as $\text{width}^2 \times \text{length} / 2$.

Histopathological Analysis

Fresh mice tissues were fixed with 4% paraformaldehyde and embedded in paraffin. The paraffin-embedded block tissues were cut into 4 μ m sections and the positive expression of the cleaved caspase-3 (Servicebio, Wuhan, China) and nuclear factor erythroid 2-related factor 2 (Nrf2) (Servicebio, Wuhan, China) were detected using a DAB Substrate kit (DAKO, Hangzhou, China), and the apoptosis level was detected using a One-Step TUNEL Apoptosis Assay Kit (Roche, Shanghai, China).

Statistical Analysis

GraphPad Prism 8 (GraphPad Software, Inc.) was used for statistical analysis. These were expressed as mean \pm standard deviation (SD), and were analyzed through one-way analysis of variance (ANOVA) followed by the least significant difference or the Dunnett's T3 test. Statistically significant differences were considered when $P < 0.05$.

Results

β -Mangostin Inhibits Viability of Glioma Cells

The main compound from *Garcinia mangostana* L. structure was identified by nuclear magnetic resonance spectroscopy (Supplementary materials Table 1 and Figures 1–3) and literature data comparison in confirming β -mangostin.

The effect of β -mangostin on C6 cell viability was assessed using the MTS assay, clone formation experiment, and cell scratch test. The main extract (SZ) and its six components were screened using the MTS assay. It was found that the extract (SZ) and the third component (SZ3) had a significant

inhibitory effect on glioma cells (Figure 1A). β -Mangostin, the main component of SZ3 (Figure 1B), was tested further with CCK-8 assay (Figure 1C), and the inhibitory effect on glioma cells with an IC₅₀ of approximately 4.811 μ M was observed. In addition, we also verified the proliferation of different cell lines and found that the 50% inhibition rate of U251 and T89G cells was 5.831 μ M and 10.320 μ M (Supplementary materials Table 2).

According to the clone formation and cell scratch experiment (Figure 1D–F), β -mangostin treatment inhibited the growth of C6 cells in a concentration-dependent manner. When β -mangostin concentration exceeded 6 μ M, both colony formation rate and cell proliferation rate were significantly reduced compared with those in the control group.

β -Mangostin Induces ROS Generation and Decreases Mitochondrial Membrane Potential

The mitochondrial membrane potential was detected using the JC-1 staining method. Cells with normal mitochondria

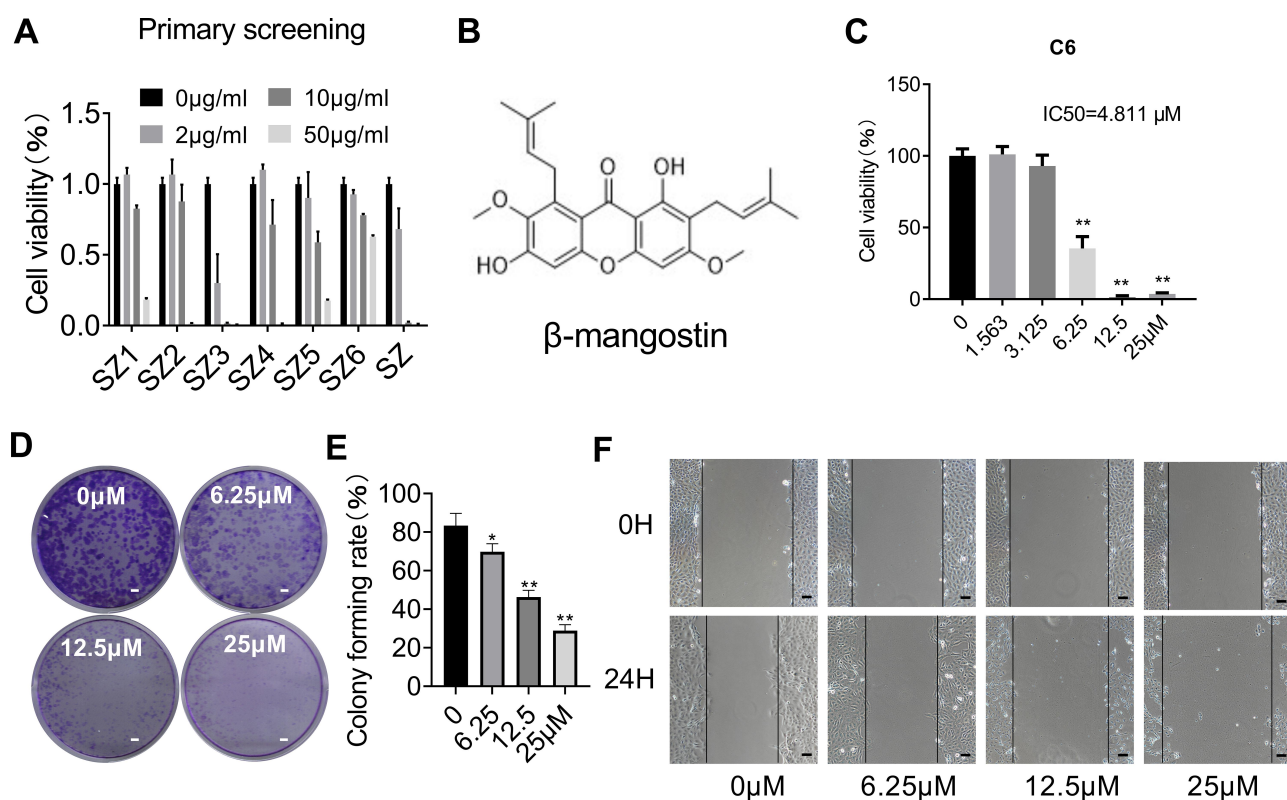


Figure 1 Effect of β -mangostin on cell proliferation in vitro. (A) CCK8 assay is conducted to measure cell viability in C6 glioma cells treated with different concentration of different fragments isolated from the shell of mangosteen. (B) The chemical structure of the main compound isolated from the SZ3 fragments. (C) CCK8 assay is conducted to measure cell viability in C6 glioma cells with different concentration of β -mangostin. (D–E) C6 cells proliferation ability is measured using clone formation assay with different concentration of β -mangostin (Scar bar: 2 mm). (F) C6 cells proliferation ability is measured using cell scratch test with different concentration of β -mangostin (Scar bar: 200 μ m). Data are the mean \pm SD for three independent experiments. ** $P < 0.01$ and * $P < 0.05$ vs. controls.

potential and depolarized mitochondria emitted red fluorescence and green fluorescence signals, respectively. The ratio of the green to red fluorescence reflected the mitochondrial depolarization. As shown in Figure 2A–C, the level of depolarized mitochondria was increased in response to β -mangostin treatment. These results suggest that β -mangostin induced mitochondria damage in C6 cells.

Afterwards, we evaluated the generation of mitochondrial ROS (MitROS) in C6 cells treated with β -mangostin. The generation of ROS was measured using the fluorescent probe DCFH-DA with a fluorescence microscope and flow cytometry. Based on Figure 2D–E, treatment with β -mangostin for 24 h resulted in an obvious and concentration-dependent rise in ROS levels in comparison with the control. The mean fluorescent intensity of DCFH-DA was significantly increased in C6 cells treated with β -mangostin using flow cytometry. The aforementioned results suggested that β -mangostin induced ROS generation. We used N-acetylcysteine to block the ROS and found that N-acetylcysteine (0.5 mM) reversed the accumulation of ROS (Supplementary materials Figure 4).

In addition, the expression of proteins related to oxidative stress was examined using Western blot analysis. Based on Figure 2F–G, the treatment of cells with β -

mangostin for 24 h increased Nrf2 level in C6 cell. These data suggest that oxidative stress may contribute to cell growth inhibition by β -mangostin in glioma cells.

Cell Cycle Arrest and Apoptosis-Inducing Effect of β -Mangostin in C6 Cells

To examine whether β -mangostin affects cell cycle progression in glioma cells, we evaluated the cell cycle phase distribution in treated cells using flow cytometry analysis. Results showed that 12.5 μ M of β -mangostin significantly arrested cell cycle progression in C6 cells by decreasing the percentage of cells in the G1 phase ($63.64\% \pm 0.69\%$ compared with $72.71\% \pm 0.75\%$ in the control group). It also increased the percentage of cells in the S phase ($27.67\% \pm 1.92\%$ compared with $15.88\% \pm 1.21\%$ in the control group) (Figure 3A and B).

In addition, flow cytometry analysis was performed to determine whether cell growth inhibition by β -mangostin was through apoptosis. As shown in Figure 3C and D, the treatment of C6 cells with various doses of β -mangostin for 24 h induced cell apoptosis in a dose-dependent manner, especially for late-stage apoptosis. Briefly, β -mangostin

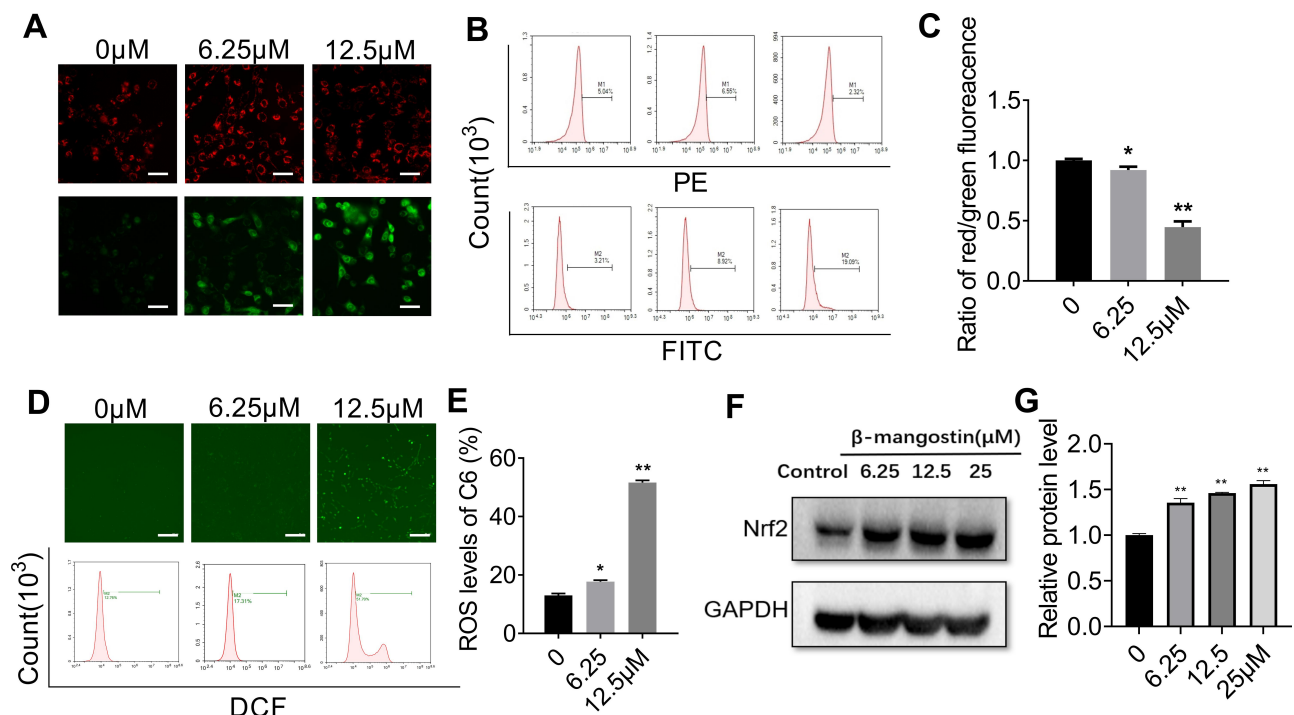


Figure 2 Effect of β -mangostin on oxidative stress in glioma cells. C6 cells are treated with two concentrations of β -mangostin (6.25 and 12.5 μ M). (A–C) The mitochondrial membrane potential in C6 cells is detected using fluorescence microscopy and flow cytometry (Scar bar:500 μ m). (D–E) The active oxygen levels in C6 cells is detected using fluorescence microscopy and flow cytometry (Scar bar:2 mm). (F–G) The oxidative stress relevant protein (Nrf2) levels in C6 is detected using Western blotting. Data are the mean \pm SD for three independent experiments. ** $P < 0.01$ and * $P < 0.05$ vs. controls.

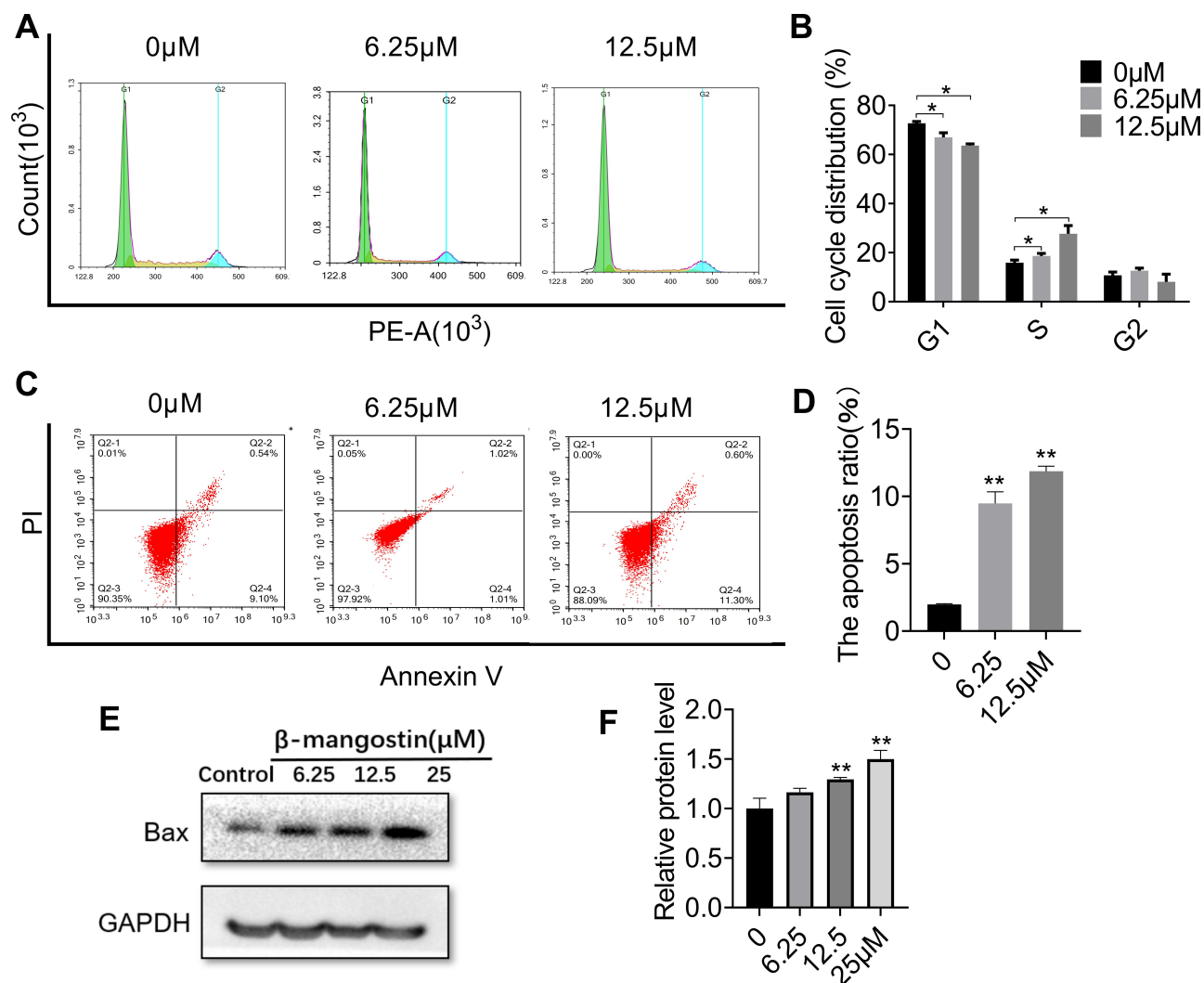


Figure 3 Effect of β -mangostin on apoptosis in glioma cells. C6 cells are treated with two concentrations of β -mangostin (6.25 and 12.5 μ M). (A-B) C6 cells cycle phase distribution is measured using flow cytometry. (C-D) C6 cells apoptosis is measured using flow cytometry. (E-F) The expression of Bax in C6 is measured using Western blotting. Data are the mean \pm SD for three independent experiments. ** P <0.01 and * P <0.05 vs. controls.

treatment led to an increased cell apoptotic rate from 1.98% \pm 0.05% in the control group to 10.22% \pm 0.58% (1 μ g/mL) and 11.86% \pm 0.36% (2 μ g/mL) in C6 cells. Afterwards, the expression of proteins related to apoptosis was examined using Western blot analysis. Treatment with β -mangostin for 24 h increased Bax level in C6 cell. These data suggest that apoptosis may contribute to cell growth inhibition by β -mangostin in glioma cells (see Figure 3E and F).

PI3K/AKT/mTOR Pathway is Involved in the Anticancer Effect of β -Mangostin in Glioma Cells

PI3K/AKT/mTOR signaling pathways have been shown to play essential roles in glioma. Hence, we explored the

effect of the β -mangostin treatment in glioma cells with this pathway. We determined the inhibitory effects of β -mangostin on the PI3K/AKT pathway and found that 12.5 μ M of β -mangostin obviously repressed the phosphorylation of PI3K and AKT (S473). Meanwhile, the phosphorylation of downstream proteins, such as mTOR, was substantially suppressed compared with the control group (Figure 4A and B). Afterwards, we added the PI3K inhibitor, LY294002 (25 μ M). As shown in Figure 4C and D, LY294002 treatment decreased the levels of p-AKT and p-mTOR. Moreover, β -mangostin further enhanced the inhibition of this pathway by LY294002 after the combined treatment with β -mangostin (6.25 μ M) and LY294002 (25 μ M).

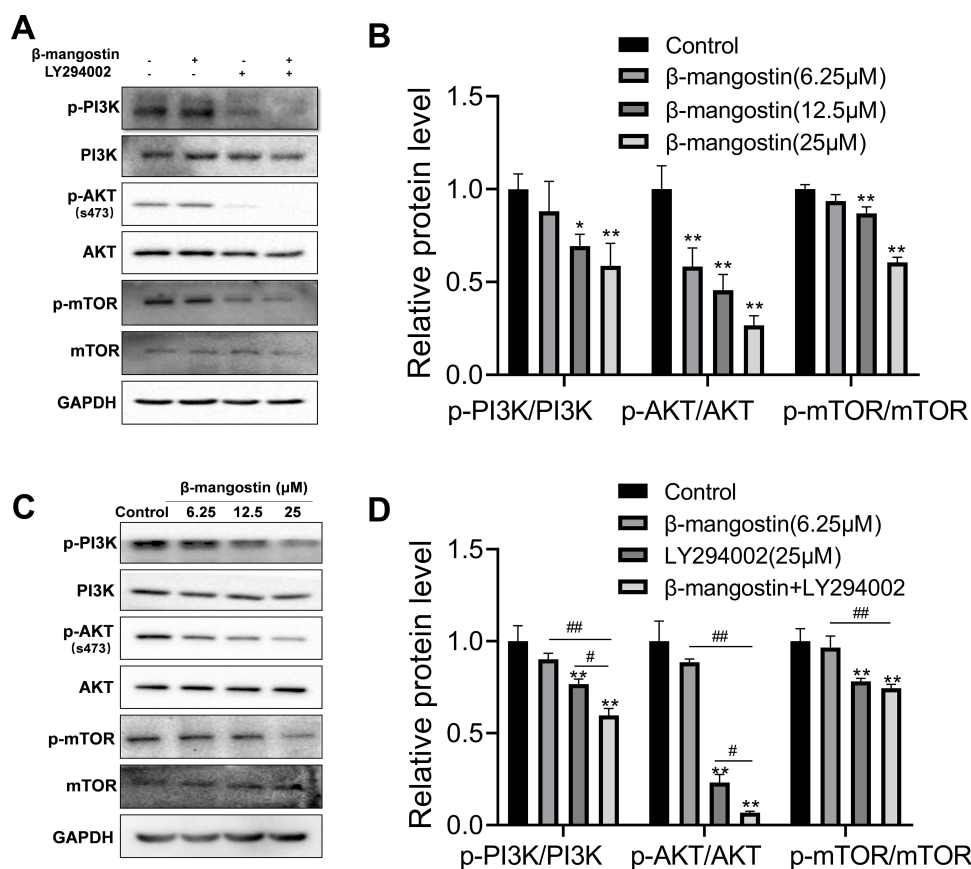


Figure 4 Role of β -mangostin on PI3K/AKT/mTOR pathway regulation in glioma. C6 cells were pretreated with three concentrations of β -mangostin (6.25, 12.5, and 25 μ M). (A-B) Western blot analysis of PI3K/AKT/mTOR pathway in C6 cells. (C-D) Western blot analysis of PI3K/AKT/mTOR pathway after adding the PI3K inhibitor, LY294002 in C6 cells. Data are the mean \pm SD for three independent experiments. ** $P < 0.01$ and * $P < 0.05$ vs. controls. ### $P < 0.01$ and # $P < 0.05$ vs. " β -mangostin+LY294002."

β -Mangostin Inhibited Tumor Growth in C6 Xenograft Tumor Models

To further validate the results of in vitro experiments on the tumor growth inhibition, C6 xenograft tumor models were used to probe the inhibitory effects of β -mangostin. As shown in Figure 5A and B, tumor volumes were substantially lower in mice treated with β -mangostin than the control group. Treatment with β -mangostin did not cause any signs of toxicity or significantly alteration of mice body weight (Figure 5C). The immunohistochemistry assay showed that the expression levels of cleaved caspase-3 and Nrf2 were decreased by the treatment of β -mangostin (Figure 5D). Similarly, the TUNEL assay demonstrated that the number of apoptotic cells increased in the tumor tissue (Figure 5E).

Discussion

Mangosteen is a fruit that mainly grows in Thailand, Vietnam, and other tropical countries. Its nutshell has been used as a natural medicine for dysentery, ulcers, wound

infection, typhoid fever, and antibacterial disinfection.¹² Among the bioactive compounds isolated from mangosteen, xanthone derivatives, mainly including α -mangostin, β -mangostin, and γ -mangostin, have been widely reported to have antitumor biological effects in several cancers, such as hepatocarcinoma, lung cancer, and breast cancer.^{18,23–25} It was reported that α -mangostin glycosides might be potential anti-hepatocarcinoma agents that can downregulate VEGF and HiF-1 α via c-Met signal pathway.²⁶ Another report had shown that antitumor and metastatic effects of β -mangostin in cervical cancer were mediated through JNK2/AP-1/Snail cascade.²⁷ In this study, we demonstrated that the major component of *Garcinia mangostana* L. extract, β -mangostin, could cause the C6 oxidative damage-induced cell death in glioma cells through PI3K/AKT/mTOR pathway inhibition.

PI3K/AKT is a potent pathway to activate and trigger cell survival signals, which play a crucial role in apoptotic cell death associated with chemotherapeutic drug treatment.^{28,29} Dysregulation of this pathway is also related to the

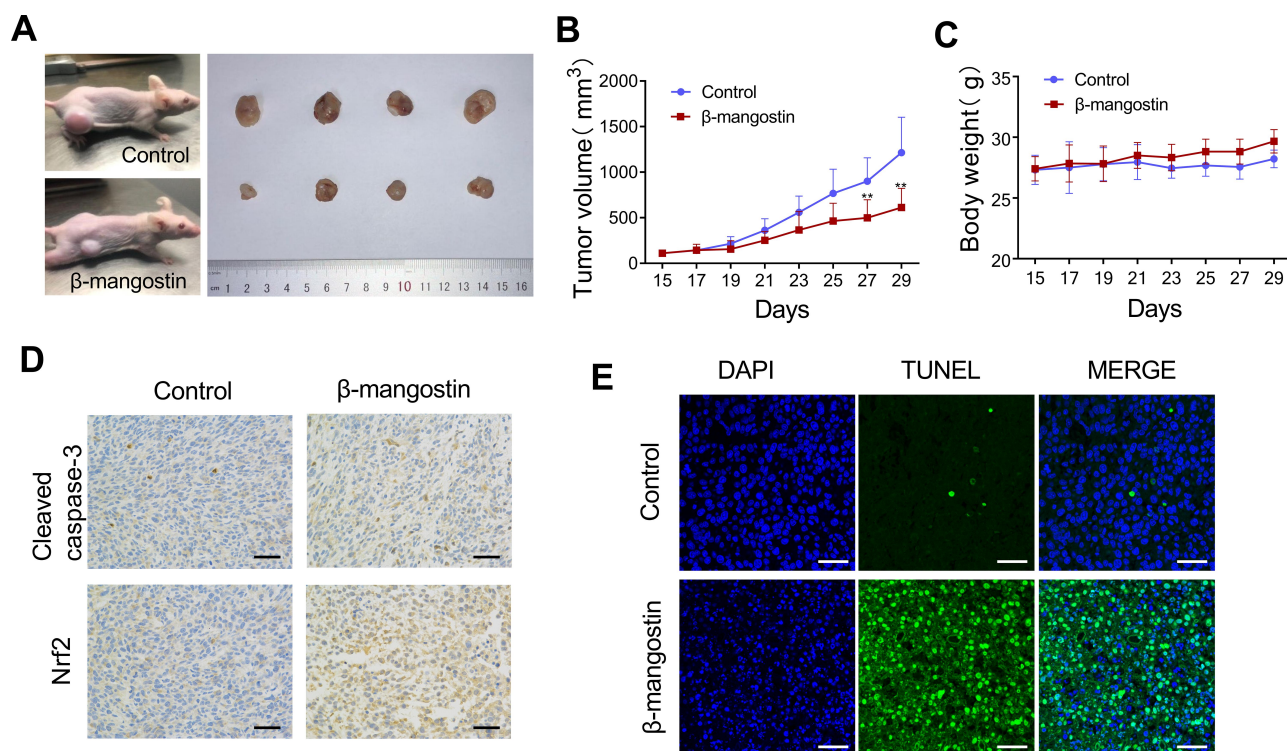


Figure 5 β -mangostin inhibits growth of glioma cells in vivo. Subcutaneous transplantation tumor model of C6 cells is conducted to determine the effect of β -mangostin in vivo. (A) Schematic diagram of tumors in treatment group and control group on day 29. (B-C) Tumor volume and body weight in mice comparing between the treatment and control groups. (D) Immunohistochemical detection of Cleaved Caspase-3 and Nrf2 protein levels in the tumor tissues (Scar bar:500 μ m). (E) TUNEL immunofluorescence method to detect the apoptosis of tumor tissue (Scar bar:200 μ m). Data are the mean \pm SD for three independent experiments. ** P <0.01 vs. controls.

therapeutic resistance of glioma.³⁰ With that, our results demonstrated that β -mangostin resulted in a significant induction of apoptosis and in a concomitant reduction of Akt phosphorylation at Ser473, which consequently inhibited PI3K/AKT/mTOR signaling pathway in C6 cells. In addition, flow cytometry analysis indicated that treatment of C6 cells with β -mangostin resulted in a significant induction of apoptosis. Induction of apoptosis in tumor cells is considered to act as a protective mechanism that inhibits neoplastic development by eliminating the cells that have been improperly stimulated for proliferation.^{31,32} LY294002 (2-4-morpholinyl-8-phenylchromone) is a chemical inhibitor of PI3K that is used extensively to study the role of the PI3K/Akt pathway in normal and transformed cells.^{33,34} Our results confirmed that β -mangostin with PI3K broad-spectrum inhibitor LY294002 could further decrease the phosphorylation of Akt in C6 cells. Furthermore, our findings indicate that the inhibition of glioma cell proliferation by β -mangostin is in part due to suppression of PI3K/Akt/mTOR signaling and β -mangostin appears to be a potent chemotherapeutic agent against glioma cells.

We also found that when cells were incubated with β -mangostin, ROS generation was increased and the

mitochondrial membrane potential was changed, which was reflected by the significant increase in FITC levels, a significant decrease in the PE levels, and increase in Nrf2 protein levels. Since cancer cells have a special redox state, which is mostly elevated with ROS generation, ROS damage may be exploited for therapeutic purposes to induce cancer cell death while sparing normal cells.³⁵ Recent signs of progress in cancer research suggest that intracellular ROS generation through oxidative stress is a common pathway of cancer cell cytotoxicity and apoptosis.^{36,37} An imbalance between the production of ROS and cells antioxidant system's ability to readily detoxify ROS, results in oxidative stress.^{38,39} It was shown that ROS released during quercetin and chloroquine administration resulted in caspase activation which was particularly involved in the survival of glioma cells.⁴⁰ In addition, mitochondria-mediated apoptosis was accompanied by BAX mitochondrial distribution and oligomerization, and caspase 3/caspase 8/caspase 9 activation.⁴¹ This finding is consistent with our current results showing that the cleaved-caspase 3 activated and PI3K/AKT/mTOR signaling pathway were inhibited by the β -mangostin treatment.

Although in vitro cell culture models are a good method for preliminary screening of chemotherapeutic drug effects, results must be verified in vivo using animal models before considering human trials. Lee et al demonstrated that α -mangosteen extracted from the pericarp of the mangosteen fruit inhibited the growth of tongue mucoepidermoid carcinoma cells in vitro and in vivo using murine ectopic xenografts models.⁸ We also used in vivo xenograft mice model inoculating C6 tumor cells in athymic nude mice to verify the chemotherapeutic potential of β -mangostin treatment against glioma tumor cell growth. Our experiment provided evidence that β -mangostin administration via tail vein injection at 5 mg/kg dosages significantly inhibited the growth of C6 tumor xenografts. Moreover, tumor xenograft growth inhibition in BALB/c nude mice by injecting β -mangostin was also associated with the induction of apoptotic cell death in C6 cells, as indicated by the TUNEL-positive and activated caspase-3-positive cells in xenograft tissues.

Conclusion

Results demonstrated that β -mangostin treatment inhibition of cell proliferation in rat C6 glioma cells depended on oxidative stress induction via PI3K/AKT/mTOR pathway inhibition. β -Mangostin administration was found to induce cell migration and apoptosis. Therefore, these findings support the possibility of β -mangostin as a potential treatment for glioma.

Acknowledgments

We are deeply grateful to Professor Youmin Ying for his assistance in β -mangostin extraction.

Funding

This work was supported by grants from Key projects jointly constructed by the Ministry and the province of Zhejiang Medical and Health Science and Technology Project (WKJ-ZJ-2019). Key and Major Projects of Traditional Chinese Medicine Scientific Research Foundation of Zhejiang Province (2019ZZ001, 2018ZY001). The National Natural Science Foundation of Zhejiang Province (LQ17H160017).

Disclosure

Zhen Wang reports a patent licensed for Method for anticancer drug. The authors report no other potential conflicts of interest in this work.

References

1. Wirsching HG, Galanis E, Weller M. Glioblastoma. *Handb Clin Neurol*. 2016;134:381–397. doi:10.1016/B978-0-12-802997-8.00023-2
2. Ellison DW. Multiple molecular data sets and the classification of adult diffuse gliomas. *N Engl J Med*. 2015;372(26):2555–2557. doi:10.1056/NEJMe1506813
3. Park DM, Sathornsumetee S, Rich JN. Medical oncology: treatment and management of malignant gliomas. *Nat Rev Clin Oncol*. 2010;7(2):75–77. doi:10.1038/nrclinonc.2009.221
4. Hombach-Klonisch S, Mehrpour M, Shojaei S, et al. Glioblastoma and chemoresistance to alkylating agents: involvement of apoptosis, autophagy, and unfolded protein response. *Pharmacol Ther*. 2018;184:13–41. doi:10.1016/j.pharmthera.2017.10.017
5. Tavana E, Mollazadeh H, Mohtashami E, et al. Quercetin: a promising phytochemical for the treatment of glioblastoma multiforme. *BioFactors*. 2020;46(3):356–366. doi:10.1002/biof.1605
6. Afshari A, Mollazadeh H, Mohtashami E, et al. Protective role of natural products in glioblastoma multiforme: a focus on nitric oxide pathway. *Curr Med Chem*. 2020;27. doi:10.2174/0929867327666200130104757.
7. Suthamarak W, Numpraphrut P, Charoensakdi R, et al. Antioxidant-enhancing property of the polar fraction of mangosteen pericarp extract and evaluation of its safety in humans. *Oxid Med Cell Longev*. 2016;2016:1293036. doi:10.1155/2016/1293036
8. Murakami M. Antitumor and apoptosis-inducing effects of α -mangostin extracted from the pericarp of the mangosteen fruit (*Garcinia mangostana* L.) in YD-15 tongue mucoepidermoid carcinoma cells. *Int J Mol Med*. 2016;37(4):939–948. doi:10.3892/ijmm.2016.2517.
9. Wu C, Hsiao S, Murakami M, et al. Alpha-mangostin reverses multidrug resistance by attenuating the function of the multidrug resistance-linked ABCG2 transporter. *Mol Pharm*. 2017;14(8):2805–2814. doi:10.1021/acs.molpharmaceut.7b00334
10. Ghasemzadeh A, Jaafar HZE, Baghdadi A, Tayebi-Meigooni A. Alpha-mangostin-rich extracts from mangosteen pericarp: optimization of green extraction protocol and evaluation of biological activity. *Molecules*. 2018;23(8):8. doi:10.3390/molecules23081852
11. Zhang X, Liu J, Yong H, Qin Y, Liu J, Jin C. Development of antioxidant and antimicrobial packaging films based on chitosan and mangosteen (*Garcinia mangostana* L.) rind powder. *Int J Biol Macromol*. 2020;145:1129–1139. doi:10.1016/j.ijbiomac.2019.10.038
12. Lee Y, Kim S, Oh Y, et al. γ inhibition of oxidative neurotoxicity and scopolamine-induced memory impairment by β -mangostin: and evidence. *Oxid Med Cell Longev*. 2019;2019:3640753. doi:10.1155/2019/3640753
13. Chae H-S, Oh S-R, Lee H-K, Joo SH, Chin Y-W. Mangosteen xanthones, α - and γ -mangostins, inhibit allergic mediators in bone marrow-derived mast cell. *Food Chem*. 2012;134(1):397–400. doi:10.1016/j.foodchem.2012.02.075
14. Yin Q, Wu Y, Pan S, et al. Activation of Cholinergic anti-inflammatory pathway in peripheral immune cells involved in therapeutic actions of α -mangostin on collagen-induced arthritis in rats. *Drug Des Devel Ther*. 2020;14:1983–1993. doi:10.2147/ddt.S249865
15. Chiu Y, Wu J, Yeh C, Yadav V, Huang H, Wang LJA. *Garcinia mangostana* γ -mangostin isolated from L. suppresses inflammation and alleviates symptoms of osteoarthritis via modulating miR-124-3p/IL-6/NF- κ B signaling. *Aging*. 2020;12(8):6630–6643. doi:10.18632/aging.103003
16. Widayarnan AS, Lay SH, Wendhita IP, Tjakra EE, Murdono FI, Binartha CTO. Indonesian mangosteen fruit (*Garcinia mangostana* L.) peel extract inhibits *Streptococcus mutans* and *Porphyromonas gingivalis* in biofilms in vitro. *Contemp Clin Dent*. 2019;10(1):123–128. doi:10.4103/ccd.ccd_758_18

17. Tarasuk M, Songprakhon P, Chimma P, Sratongno P, Na-Bangchang K, Yenchitsomanus P. Alpha-mangostin inhibits both dengue virus production and cytokine/chemokine expression. *Virus Res.* 2017;240:180–189. doi:10.1016/j.virusres.2017.08.011
18. Huang CF, Teng YH, Lu FJ, et al. β -mangostin suppresses human hepatocellular carcinoma cell invasion through inhibition of MMP-2 and MMP-9 expression and activating the ERK and JNK pathways. *Environ Toxicol.* 2017;32(11):2360–2370. doi:10.1002/tox.22449
19. Lee K, Ryu H, Oh S, et al. Depigmentation of α -melanocyte-stimulating hormone-treated melanoma cells by β -mangostin is mediated by selective autophagy. *Exp Dermatol.* 2017;26(7):585–591. doi:10.1111/exd.13233
20. Lin C, Lin C, Ying T, et al. β -Mangostin inhibits the metastatic power of cervical cancer cells attributing to suppression of JNK2/AP-1/Snail cascade. *J Cell Physiol.* 2020;235(11):8446–8460. doi:10.1002/jcp.29688
21. Jalili-Nik M, Sadeghi M, Mohtashami E, et al. Zerumbone promotes cytotoxicity in human malignant glioblastoma cells through reactive oxygen species (ROS) generation. *Oxid Med Cell Longev.* 2020;2020:3237983. doi:10.1155/2020/3237983
22. Kim S. Beta-mangostin from *Cratoxylum arborescens* activates the intrinsic apoptosis pathway through reactive oxygen species with downregulation of the HSP70 gene in the HL60 cells associated with a G/G cell-cycle arrest. *Tumour Biol.* 2017;39(11):1010428317731451. doi:10.1177/1010428317731451
23. Phan TKT, Shahbazzadeh F, Pham TTH, Kihara T. Alpha-mangostin inhibits the migration and invasion of A549 lung cancer cells. *PeerJ.* 2018;6:e5027. doi:10.7717/peerj.5027
24. Scolamiero G, Pazzini C, Bonafe F, Guarnieri C, Muscari C. Effects of alpha-mangostin on viability, growth and cohesion of multicellular spheroids derived from human breast cancer cell lines. *Int J Med Sci.* 2018;15(1):23–30. doi:10.7150/ijms.22002
25. Yan XT, Sun YS, Ren S, et al. Dietary alpha-mangostin provides protective effects against acetaminophen-induced hepatotoxicity in mice via Akt/mTOR-mediated inhibition of autophagy and apoptosis. *Int J Mol Sci.* 2018;19:5. doi:10.3390/ijms19051335
26. Kim SM, Han JM, Le TH, Sohng JK, Jung HJ. Anticancer and antiangiogenic activities of novel α -mangostin glycosides in human hepatocellular carcinoma cells via downregulation of c-Met and HIF-1 α . *Int J Mol Sci.* 2020;21(11). doi:10.3390/ijms21114043
27. Kim S, et al. β -Mangostin inhibits the metastatic power of cervical cancer cells attributing to suppression of JNK2/AP-1/Snail cascade. *J Cell Physiol.* 2020. doi:10.1002/jcp.29688
28. Wei M, Wu Y, Liu H, Xie C, Xie C. Genipin induces autophagy and suppresses cell growth of oral squamous cell carcinoma via PI3K/AKT/MTOR pathway. *Drug Des Devel Ther.* 2020;14:395–405. doi:10.2147/ddt.S222694
29. Liu H. A novel derivative of valepotriate inhibits the PI3K/AKT pathway and causes Noxa-dependent apoptosis in human pancreatic cancer cells. *Acta Pharmacol Sin.* 2020. doi:10.1038/s41401-019-0354-1
30. Zhu Y, Liu X, Zhao P, Zhao H, Gao W, Wang L. pharmacology WLJFi. Celastrol suppresses glioma vasculogenic mimicry formation and angiogenesis by blocking the PI3K/Akt/mTOR signaling pathway. *Front Pharmacol.* 2020;11:25. doi:10.3389/fphar.2020.00025
31. Sithara T, Dhanya BP, Arun KB. Zerumbone, a cyclic sesquiterpene from *Zingiber zerumbet* induces apoptosis, cell cycle arrest, and antimigratory effects in SW480 colorectal cancer cells. *J Agric Food Chem.* 2018;66(3):602–612. doi:10.1021/acs.jafc.7b04472
32. Afshari A, Mollazadeh H, Henney N, Jamialahmad T, Sahebkar A. Effects of statins on brain tumors: a review. *Semin Cancer Biol.* 2020. doi:10.1016/j.semcancer.2020.08.002
33. Wu J, Ni Y, Yang Q. Long-term arsenite exposure decreases autophagy by increased release of Nrf2 in transformed human keratinocytes. *Sci Total Environ.* 2020;734:139425. doi:10.1016/j.scitotenv.2020.139425
34. Jiang H, Fan D, Zhou G, Li X, Deng H. Phosphatidylinositol 3-kinase inhibitor(LY294002) induces apoptosis of human nasopharyngeal carcinoma in vitro and in vivo. *J Exp Clin Cancer Res.* 2010;29(1):34. doi:10.1186/1756-9966-29-34
35. Wang G, Zhang T, Sun W. Arsenic sulfide induces apoptosis and autophagy through the activation of ROS/JNK and suppression of Akt/mTOR signaling pathways in osteosarcoma. *Free Radic Biol Med.* 2017;106:24–37. doi:10.1016/j.freeradbiomed.2017.02.015
36. Raj RK. beta-Sitosterol-assisted silver nanoparticles activates Nrf2 and triggers mitochondrial apoptosis via oxidative stress in human hepatocellular cancer cell line. *J Biomed Mater Res A.* 2020. doi:10.1002/jbm.a.36953
37. Vairavel M, Devaraj E, Shanmugam R. An eco-friendly synthesis of Enterococcus sp.-mediated gold nanoparticle induces cytotoxicity in human colorectal cancer cells. *Environ Sci Pollut Res Int.* 2020;27(8):8166–8175. doi:10.1007/s11356-019-07511-x
38. Sharma V, Joseph C, Ghosh S, Agarwal A, Mishra MK, Sen E. Kaempferol induces apoptosis in glioblastoma cells through oxidative stress. *Mol Cancer Ther.* 2007;6(9):2544–2553. doi:10.1158/1535-7163.Mct-06-0788
39. Liu H. Chidamide inhibits glioma cells by increasing oxidative stress via the miRNA-338-5p regulation of Hedgehog signaling. *Oxid Med Cell Longev.* 2020;2020:7126976. doi:10.1155/2020/7126976
40. Jang E, Kim IY, Kim H. Quercetin and chloroquine synergistically kill glioma cells by inducing organelle stress and disrupting Ca homeostasis. *Biochem Pharmacol.* 2020;178:114098. doi:10.1016/j.bcp.2020.114098
41. Chang C. Aspirin induced glioma apoptosis through noxa upregulation. *Int J Mol Sci.* 2020;21:12. doi:10.3390/ijms21124219

Drug Design, Development and Therapy

Dovepress

Publish your work in this journal

Drug Design, Development and Therapy is an international, peer-reviewed open-access journal that spans the spectrum of drug design and development through to clinical applications. Clinical outcomes, patient safety, and programs for the development and effective, safe, and sustained use of medicines are a feature of the journal, which has also

been accepted for indexing on PubMed Central. The manuscript management system is completely online and includes a very quick and fair peer-review system, which is all easy to use. Visit <http://www.dovepress.com/testimonials.php> to read real quotes from published authors.

Submit your manuscript here: <https://www.dovepress.com/drug-design-development-and-therapy-journal>